

Research on Heat Transfer Law of Drilling Fluid Mixed with Low Temperature Phase Change Materials

Mu Li^{1,2,3}, Xianzhi Song¹, Hao Wang^{2,3}, Jiangshuai Wang^{4,*},
Zixiao Song⁴ and Yufei Chen^{2,3}

¹ College of Artificial Intelligence, China University of Petroleum-Beijing, Beijing, China

² CNPC Engineering Technology R&D Company Limited, Beijing, China

³ National Engineering Research Center for Oil & Gas Drilling and Completion Technology, Beijing, China

⁴ School of Petroleum and Natural Gas Engineering, Changzhou University, Changzhou, China

INFORMATION

Keywords:

Ice crystal drilling fluid
wellbore temperature control
physical simulation
phase change cooling
heat exchange performance
temperature drop amplitude

DOI: 10.23967/j.rimni.2026.10.78053

Revista Internacional
Métodos numéricos
para cálculo y diseño en ingeniería

RIMNI



UNIVERSITAT POLITÈCNICA
DE CATALUNYA
BARCELONATECH

In cooperation with
CIMNE³

Research on Heat Transfer Law of Drilling Fluid Mixed with Low Temperature Phase Change Materials

Mu Li^{1,2,3}, Xianzhi Song¹, Hao Wang^{2,3}, Jiangshuai Wang^{4,*}, Zixiao Song⁴ and Yufei Chen^{2,3}

¹College of Artificial Intelligence, China University of Petroleum-Beijing, Beijing, China

²CNPC Engineering Technology R&D Company Limited, Beijing, China

³National Engineering Research Center for Oil & Gas Drilling and Completion Technology, Beijing, China

⁴School of Petroleum and Natural Gas Engineering, Changzhou University, Changzhou, China

ABSTRACT

During the drilling process of deep and ultra-deep wells, the high-temperature wellbore environment seriously affects drilling safety and efficiency. Traditional circulating cooling methods are limited by insufficient heat exchange capacity. Therefore, this paper proposes a new active wellbore temperature control technology for drilling fluids based on the endothermic mechanism of ice crystal phase change, and builds a physical simulation experimental system to conduct a study on the influence of multiple parameters. In the experiment, pre-cooled ice crystals were added to the drilling fluid, and the influence of factors such as ice crystal size, concentration, flow rate, initial temperature of the hot fluid, viscosity of the drilling fluid, and initial temperature on the cooling performance was systematically investigated. The results show that increasing the ice crystal size and concentration can significantly improve the heat exchange effect; appropriately increasing the flow rate is beneficial to enhancing heat transfer; the higher the temperature of the hot fluid, the greater the absolute cooling amplitude, but the increase in viscosity and the initial temperature of the drilling fluid weaken the cooling effect. This study provides an experimental basis and technical support for the design and engineering application of ice crystal-type functionalized drilling fluids.

OPEN ACCESS

Received: 23/12/2025

Accepted: 12/03/2026

DOI

10.23967/j.rimni.2026.10.78053

Keywords:

Ice crystal drilling fluid
wellbore temperature control
physical simulation
phase change cooling
heat exchange performance
temperature drop amplitude

1 Introduction

Against the backdrop of the continuous transformation of the global energy structure, oil and gas resources remain an important pillar for ensuring national energy security. Despite the rapid development of new energy sources, traditional fossil fuels will still dominate the energy structure for a long time in the future [1–4]. In 2023, global oil and gas consumption accounted for more than 53% of primary energy consumption. The depletion of shallow resources has driven the exploration and development to shift towards deep (4500–6000 m) and ultra-deep (>6000 m) layers [5–8]. From 2010 to 2023, the proportion of global deep/ultra-deep oil and gas production increased from 12% to 28%, and

*Correspondence: Jiangshuai Wang (wjs125126@163.com). This is an article distributed under the terms of the Creative Commons BY-NC-SA license

it is expected to exceed 40% by 2030. China is rich in deep oil and gas resources. The geological reserves in basins such as Tarim, Sichuan, and Songliao exceed 12 billion tons of oil equivalent, accounting for more than one-third of the country's total, with huge development potential.

However, deep-well drilling faces many technical challenges, with the engineering problems caused by the extremely high-temperature environment being the most prominent [9–12]. As the well depth increases, the geothermal gradient is generally higher than 3.5 degrees Celsius per 100 m, and in some areas, the bottom-hole circulating temperature even exceeds 150 degrees Celsius. Such high temperatures not only seriously affect the performance of drilling fluids but also accelerate the aging of drilling tools and the failure rate of electronic instruments, severely restricting the safety and efficiency of drilling operations [13,14]. High temperatures can cause severe thermal degradation of water-based drilling fluids, manifested as a significant decrease in viscosity and a notable increase in fluid loss, which in turn affects well-bore stability and cuttings-carrying capacity. At the same time, metal components such as drill pipes are more prone to oxidation and corrosion at high temperatures, the wear rate of threaded connections accelerates, and the service life is significantly shortened. In addition, electronic components in downhole measurement and control systems are prone to failure in a continuous high-temperature environment, causing data transmission interruptions or logging failures, which seriously affect construction decisions [15–17]. Existing cases show that the instability of drilling fluids caused by high temperatures has led to well-bore collapse, and the economic loss of a single accident can be as high as several million yuan.

To address this challenge, the industry has successively developed various wellbore temperature control technologies. The earliest method was passive thermal insulation, which mainly involved filling high-performance thermal insulation materials between casings to slow down heat transfer [18,19]. Although it has a certain effect, it is costly and has limited insulation capacity, making it difficult to meet the needs of ultra-deep wells [20–23]. Subsequently, surface active cooling technology emerged, which introduced refrigeration equipment into the surface circulation system to cool the returned high-temperature drilling fluid before re-injecting it into the well. Although this method can achieve a certain degree of temperature control, it consumes a large amount of energy, accounting for nearly 20% of the total energy consumption of the entire drilling operation, and has poor economic efficiency [24–26]. In recent years, phase-change material temperature control technology has gradually emerged, which uses the property of substances to absorb or release a large amount of latent heat during the phase-change process to regulate temperature [27–29]. For example, paraffin-based phase-change materials have been tried in drilling fluid systems and can release cold energy downhole to achieve local cooling. However, the phase-change latent heat of such materials is relatively low, generally not exceeding 130 kJ/kg, the temperature reduction range is usually only 8 to 12 degrees Celsius, and there are problems such as poor compatibility with drilling fluids and insufficient long-term stability.

In contrast, ice crystals, as a natural phase-change medium, show unique advantages. The phase-change latent heat of water is as high as 334 kJ/kg, more than twice that of paraffin-based materials, which means that per unit mass of ice can absorb more heat during the melting process [30,31]. More importantly, ice crystals are completely compatible with water-based drilling fluids, do not introduce external chemical pollution, and are highly environmentally friendly. At the same time, their raw materials are widely available, and the preparation cost is low, only about one-twentieth of that of nano-composite phase-change materials, with good prospects for industrial application. Therefore, introducing ice crystals into the drilling fluid system and using the heat-absorption mechanism of their melting during the flow process to achieve active temperature control has become a highly promising technical approach.

The application of ice crystal drilling fluid still faces three major key technical bottlenecks. Firstly, the preparation theory is still not perfect. As a multi-component complex system containing clay, polymers, and salts, the components of the drilling fluid can affect the nucleation temperature and growth rate of ice crystals. However, there is a lack of systematic quantitative analysis and theoretical model support [32,33]. Secondly, the flow mechanism is unclear. The flow and heat transfer mechanisms of ice crystals in non-Newtonian fluids are unknown. The melting behavior in dynamic circulation is affected by the coupling of multiple factors such as flow rate, temperature field, and shear stress. In actual working conditions the optimal concentration of 5% obtained from static experiments needs to be reduced to 3% due to rapid melting, which seriously affects the temperature control efficiency. In addition, the parameter system for engineering applications has not been established. There is a lack of systematic research on the matching relationship between ice crystal size, concentration, and flow rate. Moreover, relying on externally purchased ice crystals in the early stage has problems such as inconvenient transportation and storage and high risks of ion pollution.

This paper proposes a self-freezing ice crystal phase-change temperature control technology for drilling fluid. Through an independently developed integrated experimental system of “freezing-circulation-heat transfer”, a systematic study is conducted on the preparation mechanism of ice crystals, the laws of flow and heat transfer, and the engineering applicability. The research focuses on three aspects: optimizing the ice crystal preparation process, carrying out full-scale annulus simulation experiments to explore the influence of parameters such as ice crystal size and concentration on the cooling effect of hot fluids and key parameters, and constructing a matching diagram of on-site operation parameters. Its innovation lies in putting forward the technical concept of heat absorption through ice crystal phase change, forming a complete engineering application parameter system. It is expected to provide a new solution for safe and efficient drilling in the high-temperature environment of deep and ultra-deep wells and promote the development of drilling fluid temperature control technology towards intelligence and greenness.

2 Ice Crystal Drilling Fluid Cooling Device

2.1 Overall Design of the Device

This section details the ice crystal drilling fluid cooling system used in the experiment. This system aims to simulate the cooling effect in the actual drilling process and study the influence of different parameters on the cooling efficiency by precisely controlling the experimental conditions. The experimental device consists of several key modules: the low-temperature coolant module, the heat exchanger module, the high-temperature drilling fluid module, and the computer data acquisition module. Each module is equipped with necessary high-precision instruments, such as thermometers, pressure gauges, and flow meters, to ensure the accuracy of experimental data. The inner diameter of the outer heat-exchange cylinder is set according to four aspects: the required space for temperature sensor arrangement, the outer diameter of the coil, the heat-exchange efficiency, and the hot-fluid supply capacity. The material is stainless steel according to the actual on-site application. The inner diameter of the existing experimental device is 265 mm, the wall thickness is 3 mm, the outer tube diameter is 100 mm, and there are three inner tubes with an inner diameter of 10 mm. Through this set of devices, we can simulate and study the cooling performance of ice crystal drilling fluids of different sizes under different flow rates and temperature conditions, providing a scientific basis for the design and optimization of the ground cooling system (Figs. 1–3).

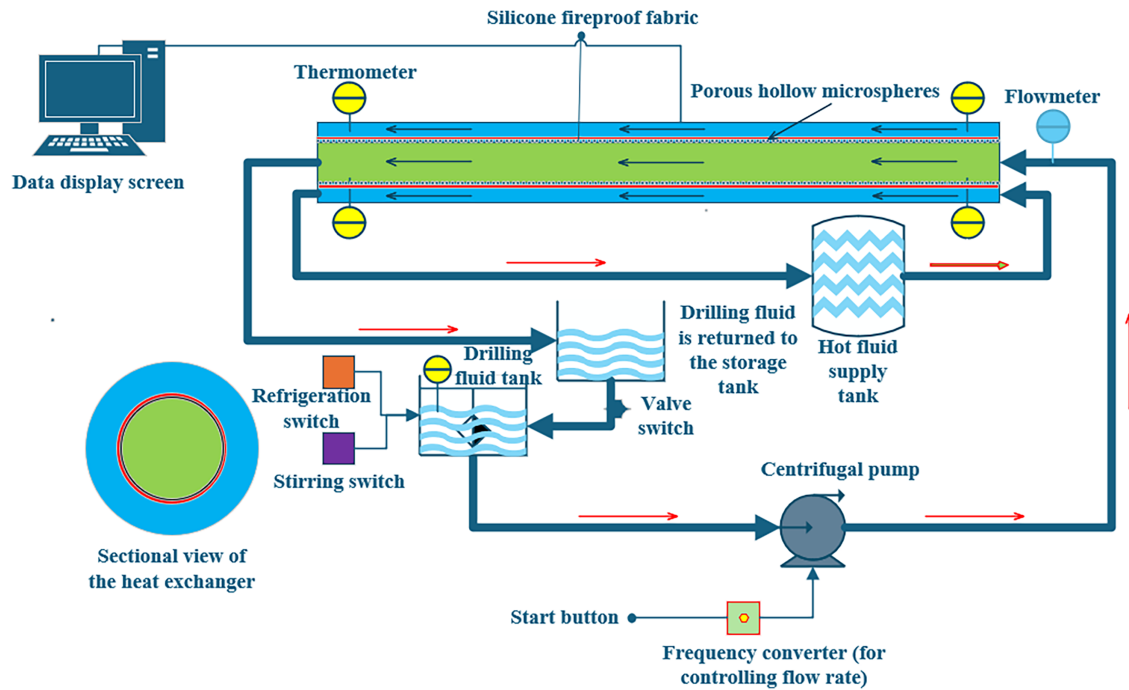


Figure 1: Schematic diagram of the cooling device for ice crystal drilling fluid



Figure 2: Ice making and ice crushing equipment



Figure 3: Physical picture of ice crystal drilling fluid cooling device

2.2 Instructions for Experimental Steps

After the installation and debugging of the experimental equipment are completed, conduct the experiment according to the following main steps (Figs. 4 and 5):

- (1) First, turn on the ice maker to start making ice. Then, use the ice crusher to make ice crystals of the corresponding size as required, and put the prepared ice crystals into the incubator.
- (2) Put the liquid to be tested into the drilling fluid tank and heat it to the predetermined temperature. Add clean water to the hot fluid supply pool and heat it to the predetermined temperature.
- (3) Add the ice crystals to the drilling fluid mixing tank, and then pump the drilling fluid into the heat exchanger at the predetermined speed. Measure the temperature values of the drilling fluid at the inlet and outlet of the heat exchanger. Use the frequency converter to control the rotation speed of the motor, thereby adjusting the flow rate of the drilling fluid. The drilling fluid flows into the drilling fluid return storage tank through the constant-flow pump.
- (4) After the experiment is completed, clean the pipelines, turn off the power supply, and process the experimental data.



Figure 4: Ice crystal sampling process

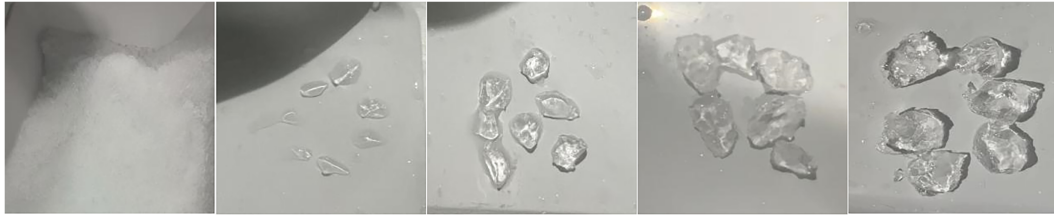


Figure 5: 1~10 mm diagrams of different ice crystal sizes

2.3 Experimental Condition Setting

In order to conduct indoor simulation experiments on cooling under various conditions such as different viscosities, flow rates, drilling fluid/coolant temperatures, ice crystal sizes and concentrations, several groups of experiments were set up in combination with the working capacity of the device. The specific conditions are detailed in [Table A1](#).

3 Research on the Experimental Laws of Ice Crystal Drilling Fluid

3.1 Physical Simulation Experiments on Wellbore Temperature Control under Different Ice Crystal Sizes

The larger the ice crystal size, the slower the melting rate and the better the heat exchange effect. Ice crystals with a concentration of 5% and a size of 9–10 mm can reduce the temperature of a hot fluid at 60°C flowing at a velocity of 1.01 m/s to 36.5°C (a temperature drop of 23.5°C) ([Fig. 6](#)).

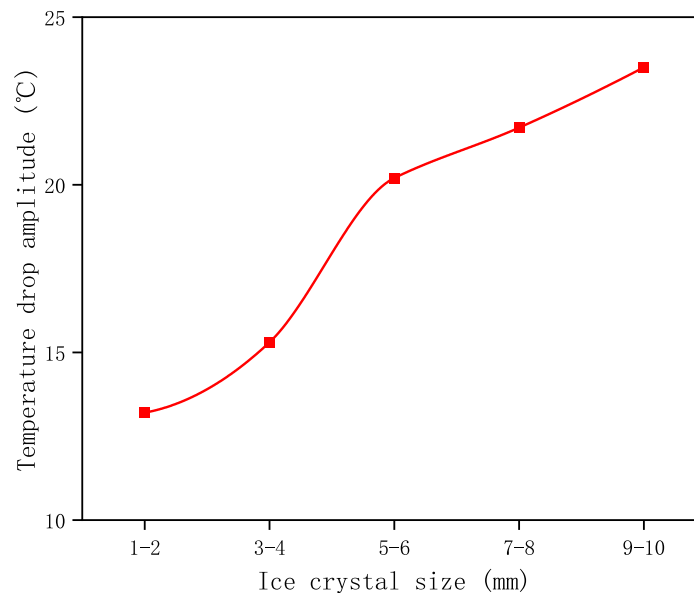


Figure 6: Under the environment of ice crystal concentration of 5%, flow velocity of 1.01 m/s, and hot fluid at 60°C

Under the conditions of an ice crystal concentration of 5%, a flow velocity of 1.01 m/s, and a hot-fluid temperature of 60°C, the experiment found that there is a positive correlation between the ice crystal size and the cooling effect. Ice crystals with a size of 1–2 mm can only achieve a temperature drop of 13.2°C, while ice crystals with a size of 9–10 mm can achieve a temperature drop of up to

23.5°C, nearly twice that of the former. This is because large ice crystals have a slower melting rate, can continuously absorb heat during the flow process, and prolong the effective cooling time.

3.2 Physical Simulation Experiments of Wellbore Temperature Control under Different Flow Rate

Under the conditions of an ice crystal concentration of 5% and an ice crystal size of 5–6 mm, a flow velocity of about 1.1 m/s can reduce the 60°C hot fluid to 36.9°C (with a temperature drop of 23.1°C) (Fig. 7).

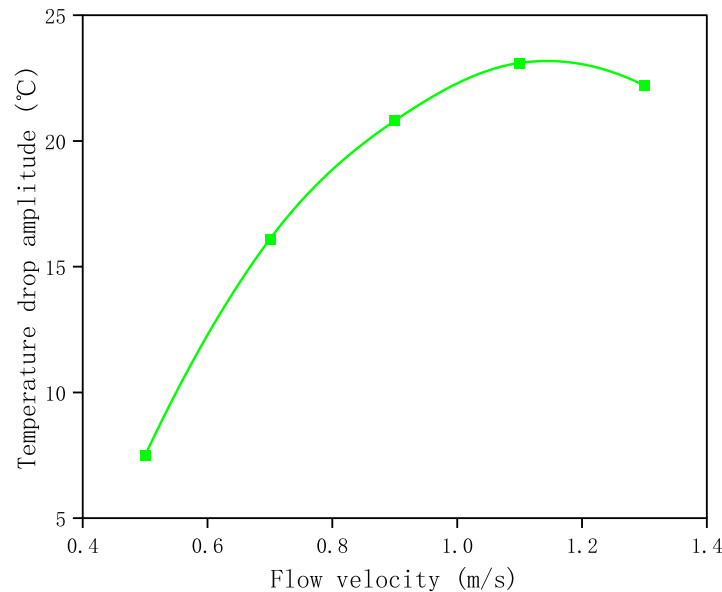


Figure 7: Ice crystal concentration of 5%, ice crystal size of 5–6 mm, under a hot fluid environment of 60°C

By adjusting the flow rate of the drilling fluid, it was found that there is a significant “optimal range” for the cooling effect. When the ice crystal concentration is 5%, the size is 5–6 mm, and the temperature of the hot fluid is 60°C, the temperature drops by 23.1°C at a flow rate of 1.1 m/s, which is the experimental peak. When the flow rate is lower than 0.8 m/s, the efficiency decreases due to insufficient processing capacity per unit time. When the flow rate is higher than 1.3 m/s, the ice crystals flow out of the heat exchange area before fully melting, resulting in a decrease in the heat absorption efficiency.

3.3 Physical Simulation Experiments on Wellbore Temperature Control under Different Ice Crystal Concentrations

Under the same flow rate, as the ice crystal concentration of the hot fluid increases, the temperature drop becomes larger and larger, and the heat transfer effect is better. With an ice crystal concentration of 20% and ice crystals with a size of 5–6 mm, the hot fluid at 60°C with a flow rate of 1.01 m/s can be cooled to 29.9°C (a temperature drop of 30.1°C) (Fig. 8).

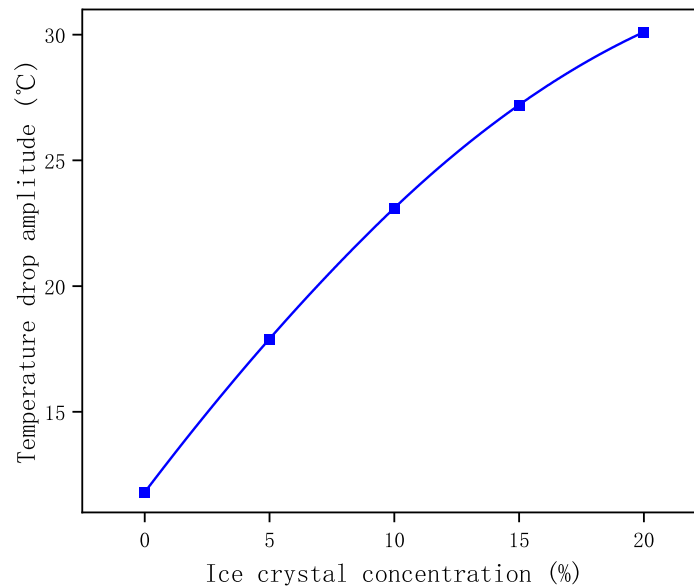


Figure 8: Flow velocity of 1.01 m/s, ice crystal size of 5–6 mm, and in a hot fluid environment at 60°C

Ice crystal concentration is the most significant factor affecting the cooling effect. Under the conditions of a size of 5–6 mm, a flow velocity of 1.01 m/s, and a hot fluid temperature of 60°C, when the concentration is increased from 0% to 20%, the cooling range increases from 7.5°C to 30.1°C. This is attributed to the fact that high-concentration ice crystals provide a larger total latent heat of phase change, enhancing the heat absorption capacity. However, it should be noted that when the concentration exceeds 20%, the viscosity of the drilling fluid increases significantly, which may affect the pumping performance. Therefore, the recommended optimal concentration is 15%–20%.

3.4 Physical Simulation Experiments on Wellbore Temperature Control under Different Hot Fluid Temperatures

As the temperature of the hot fluid continues to increase, the cooling amplitude becomes larger and larger. With an ice crystal concentration of 5% and ice crystals sized between 5–6 mm, the hot fluid at 60°C with a flow velocity of 1.01 m/s can be cooled to 37.6°C (a cooling amplitude of 22.4°C) (Fig. 9).

The influence of the hot fluid temperature on the cooling effect shows a “high-temperature amplification effect”: when the ice crystal concentration is 5%, the size is 5–6 mm, and the flow velocity is 1.01 m/s, as the hot fluid temperature rises from 40°C to 60°C, the cooling amplitude jumps from 5.5°C to 22.4°C. The stronger thermal driving force in the high-temperature environment accelerates the melting of ice crystals and heat transfer, indicating that this technology has unique advantages in ultra-high-temperature wellbores (e.g., above 60°C). The higher the temperature, the more significant the temperature control effect.

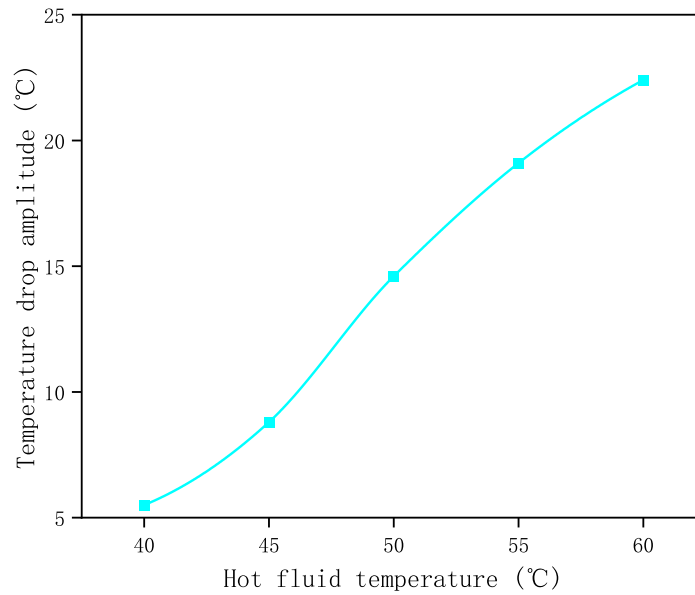


Figure 9: Under the environment of a flow velocity of 1.01 m/s, ice crystal sizes of 5–6 mm, and an ice crystal concentration of 5%

3.5 Physical Simulation Experiments on Wellbore Temperature Control under Different Viscosities

As the viscosity continuously increases, the temperature drop becomes smaller and smaller. At an ice crystal concentration of 5% and with ice crystals sized between 5–6 mm, the 60°C hot fluid flowing at a velocity of 1.01 m/s can be cooled down to 39.6°C (a temperature drop of 20.4°C) (Fig. 10).

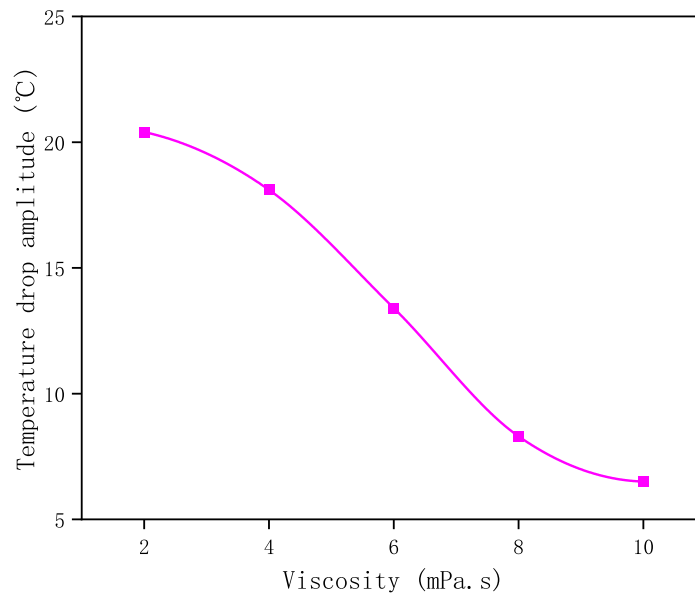


Figure 10: Under the environment of a flow velocity of 1.01 m/s, ice crystal sizes of 5–6 mm, and an ice crystal concentration of 5%

There is a negative correlation between the viscosity of drilling fluid and the cooling effect. Under the conditions of 5% ice crystal concentration, 5–6 mm size, and 60°C hot fluid, when the viscosity increases from 2 to 10 mPa·s, the cooling range decreases from 20.4°C to 18.1°C; when the viscosity further increases to 24 mPa·s, the cooling is only 6.5°C. High viscosity will hinder the uniform dispersion of ice crystals and heat convection, reducing the heat transfer efficiency.

3.6 Physical Simulation Experiments of Wellbore Temperature Control under Different Drilling Fluid Temperatures

As the temperature of the drilling fluid continues to increase, the cooling amplitude becomes smaller and smaller. With an ice crystal concentration of 5% and ice crystals sized between 5–6 mm, the 60°C hot fluid flowing at a velocity of 1.01 m/s can be cooled to 30.5°C (a cooling amplitude of 29.5°C) (Fig. 11).

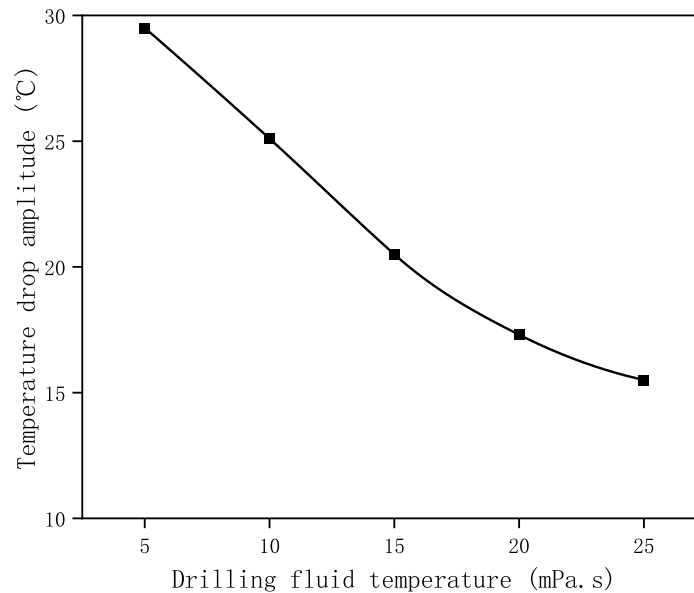


Figure 11: Under the environment of a flow velocity of 1.01 m/s, ice crystal sizes of 5–6 mm, and an ice crystal concentration of 5%

The initial temperature of the drilling fluid itself has a significant impact on the final cooling effect: when the ice crystal concentration is 5%, the size is 5–6 mm, and the temperature of the hot fluid is 60°C, as the initial temperature drops from 25°C to 5°C, the cooling amplitude increases from 15.5°C to 29.5°C, nearly doubling.

4 Analysis of Ice Crystal Model

4.1 Basic Assumptions and Physical Mechanisms

As a new type of drilling fluid system, the core mechanism of ice crystal drilling fluid lies in using the melting endothermic effect of ice crystals in the wellbore to control the wellbore temperature. This model is based on the following basic assumptions: (1) The flow of the drilling fluid in the wellbore is a steady laminar flow; (2) The main heat transfer direction is along the wellbore axis; (3) The ice crystals and the liquid phase reach local thermal equilibrium; (4) The ice crystals are uniformly distributed in the liquid phase (Table 1).

Table 1: Symbol definition

Symbol	Definition
$T_0 = 273.15 \text{ K}$	The freezing point temperature of pure water under standard atmospheric pressure
$\gamma = 0.033 \text{ J/m}^2$	Surface tension coefficient of the ice-water interface
$\rho_{ice} = 917 \text{ kg/m}^3$	Density of ice
$L = 334,000 \text{ J/kg}$	Latent heat of phase change of ice
$\beta = -0.074 \text{ K/MPa}$	Coefficient of the influence of pressure on melting point
r/m	Ice crystal radius
P	Stress
$C = 3.417 \times 10^{-6} \text{ (m/(s}\cdot\text{K))}$	Melting rate constant
T/K	Ambient temperature
$v_s/m/S$	Settling velocity
$\rho_p = \rho_{ice}$	Particle density
ρ_f	Fluid density
$d_p = 2r$	Particle diameter
μ_{eff}	Effective viscosity
$g = 9.81 \text{ m/s}^2$	Gravitational acceleration

4.2 Melting Point Temperature Correction Model

Considering the double effects of pressure and curvature, the expression for the actual melting point temperature of ice crystals is:

$$T_m(r, P) = T_0 - \frac{2\gamma T_0}{\rho_{ice} L r} + \beta P \quad (1)$$

The second term in this formula is the curvature correction term, which reflects the influence of the surface curvature effect of tiny ice crystals on the melting point; the third term is the pressure correction term, which indicates that the high-pressure environment in the deep well reduces the melting point of ice crystals.

4.3 Kinetics of Ice Crystal Melting

The rate of change of ice crystal radius with time is described by the following equation:

$$\frac{dr}{dt} = \begin{cases} -C(T - T_m) & T > T_m \\ 0 & T \leq T_m \end{cases} \quad (2)$$

4.4 Kinetics of Ice Crystal Sedimentation

Considering the particle sedimentation effect, the settling velocity of ice crystals is divided into three regions according to the particle Reynolds number:

Laminar flow region ($Re_p \leq 1$):

$$v_s = \frac{(\rho_p - \rho_f) g d_p^2}{18 \mu_{eff}} \quad (3)$$

Transition zone ($1 < Re_p \leq 2000$):

$$v_s = 0.55 \left(\frac{(\rho_p - \rho_f) g}{\rho_f} \right)^{1/2} d_p^{3/2} \mu_{eff}^{-1/2} \quad (4)$$

Turbulent flow region ($Re_p > 2000$):

$$v_s = 1.19 \left(\frac{(\rho_p - \rho_f) g d_p^2}{\rho_f} \right)^{1/3} \quad (5)$$

The particle Reynolds number is defined as: $Re_p = \frac{\rho_f d_p v}{\mu_{eff}}$, where v is the relative velocity.

4.5 Concentration Evolution Equation

The evolution equation for the ice crystal concentration considering the sedimentation and melting effects is as follows:

$$\rho_{mix} c_{p,mix} v_{inner} \frac{dT_{inner}}{dz} = UA_{inner} (T_{outer} - T_{inner}) - \rho_{ice} L \phi \frac{dr}{dt} \quad (6)$$

In the formula: $\rho_{mix} = \rho_{water}(1 - \phi) + \rho_{ice}\phi$ is the density of the mixture; $c_{p,mix} = c_{p,water}(1 - \phi) + c_{p,ice}\phi$ is the specific heat capacity of the mixture; ϕ is the volume fraction of ice crystals; U is the overall heat transfer coefficient; v_{inner} is the flow velocity in the inner tube.

$$A_{inner} = \pi D_{inner} L \quad (7)$$

Formula for the maximum temperature drop amplitude:

$$\Delta T = \frac{1}{\rho_{mix} c_{p,mix} V_{inner}} \left[UA_{inner} \int_{t_1}^{t_2} (T_{outer} - T_{inner}) dt - \rho_{ice} L \int_{t_1}^{t_2} \phi \frac{dr}{dt} dt \right] \quad (8)$$

4.6 Parameter Analysis and Boundary Conditions

The variable parameters of the model, their influencing mechanisms, and the analysis are as follows:

Ice crystal size parameter: The ice crystal radius r directly affects the melting point temperature correction term and the settling velocity. Smaller ice crystals have lower melting points and slower settling velocities. **Flow velocity parameter:** The flow velocity in the inner tube affects the heat transfer coefficient, residence time, and concentration distribution, and influences the convective heat transfer intensity through the Reynolds number. **Ice crystal concentration parameter:** The volume fraction ϕ affects the physical properties of the mixture and the latent heat of phase-change absorption. **Hot fluid temperature parameter:** The inlet temperature T_{outer} of the hot fluid in the outer tube determines the heat transfer driving force and directly affects the ice crystal melting rate. **Viscosity parameter:** The effective viscosity μ_{eff} affects the settling velocity and the heat transfer coefficient, and influences the flow regime and heat transfer performance through the Reynolds number. **Drilling fluid temperature parameter:** The inlet temperature T_{inner} of the drilling fluid in the inner tube directly affects the temperature difference from the melting point temperature and controls the melting kinetics.

The verification of some models is shown in Table 2. This model comprehensively considers multiple physical effects, such as pressure, curvature, phase change, and settlement, and the accuracy of all of them remains above 90%, indicating that the model performance is very stable, which provides theoretical guidance for the engineering application of ice crystal drilling fluid.

Table 2: Model validation

Influencing factors	Model predicted value	Experimental value	Error
Different ice crystal sizes	12.6	13.2	4.6%
	19.5	20.2	3.5%
	22.3	23.5	5.1%
Different flow velocities	7.1	7.5	5.3%
	19.9	20.8	4.3%
	21.6	22.2	2.7%
Different ice crystal concentrations	11.1	11.8	5.9%
	22.5	23.1	2.6%
	29.2	30.1	3.0%
Different hot fluid temperatures	5.2	5.5	5.5%
	13.9	14.6	4.8%
	21.6	22.4	3.6%
Different drilling fluid temperatures	19.6	20.4	3.9%
	12.8	13.4	4.5%
	6.1	6.5	6.1%

5 Conclusions and Insights

- (1) This study successfully proposed and verified the feasibility and effectiveness of the “self-freezing ice crystal phase-change temperature control technology for drilling fluids”. By constructing a physical simulation experimental system integrating ice-making, circulation, heat exchange, and data acquisition, the influence laws of key parameters such as ice crystal size, concentration, flow rate, hot fluid temperature, drilling fluid viscosity, and initial temperature on the cooling performance were systematically investigated. The experimental results show that the endothermic mechanism of ice crystal phase-change can significantly reduce the temperature of high-temperature drilling fluids, and under specific parameter combinations, it exhibits far greater thermal management potential than traditional cooling methods. This technology fully utilizes the high latent heat of phase-change of water and the high compatibility with the drilling fluid system, achieving green, efficient, and low-cost active temperature control, and providing a new solution to the high-temperature problem in deep and ultra-deep wells.

- (2) The study further revealed the mechanism of action of each parameter on the cooling effect: increasing the ice crystal concentration and size helps to improve the total heat absorption and melting duration, thereby enhancing the temperature control ability; appropriately increasing the flow rate can optimize the heat transfer efficiency, but an excessively high flow rate will cause the ice crystals to be carried out of the heat-exchange area before being fully melted; in a high-temperature hot fluid environment, the cooling amplitude is significantly increased due to the enhanced thermal driving force, which reflects the “high-temperature amplification effect”; while an increase in drilling fluid viscosity or initial temperature inhibits the heat transfer process and reduces the cooling efficiency. Based on the multi-parameter coupling analysis, this paper preliminarily established suggestions for the process window of temperature control of ice-crystal drilling fluids, it is recommended to apply within specific ranges of particle size, concentration, and flow rate, and to use it preferentially under working conditions with a lower initial drilling fluid temperature and a higher hot fluid temperature to maximize the benefits of phase-change cooling.
- (3) Engineering feasibility outlook: In response to the engineering implementation challenges of the “self-freezing ice crystal” technology, three aspects of research need to be focused on for breakthroughs in the future. Firstly, energy consumption optimization. Explore the possibility of using the waste heat from well sites or renewable energy to drive the ice-making system, so as to reduce the additional energy consumption of ground ice-making. Secondly, system integration. Simplify the on-site deployment and maintenance processes of the circulation system through modular design, and balance complexity and reliability. Thirdly, a continuous operation guarantee. Develop real-time monitoring and automatic replenishment devices for ice crystal concentration to ensure the stability of the cooling performance during long-term drilling operations. Breakthroughs in the above directions will lay the foundation for the technology to move from the laboratory to industrial applications.

Acknowledgement: Not applicable.

Funding Statement: This research work was supported by the National Science and Technology Major Project (No. 2025ZD1402000, No. 2025ZD1402002), the Youth Science and Technology Program of China National Petroleum Corporation (2024DQ03086), and the National Natural Science Foundation of China (No. U24B2030).

Author Contributions: The authors confirm contribution to the paper as follows: study conception and design: Mu Li, Hao Wang; data collection: Jiangshuai Wang, Xianzhi Song; analysis and interpretation of results: Zixiao Song; draft manuscript preparation: Yufei Chen. All authors reviewed and approved the final version of the manuscript.

Availability of Data and Materials: The datasets generated during and/or analyzed during the current study are available from the corresponding author on reasonable request.

Ethics Approval: Not applicable.

Conflicts of Interest: The authors declare no conflicts of interest.

Appendix A

Table A1: Number of experimental groups and experimental conditions

Viscosity	Drilling fluid temperature	Heat source temperature	Flow velocity	Ice crystal size	Ice crystal concentration
1 mPa·s	10°C	60°C	1.01 m/s	1–2 mm	5%
1 mPa·s	10°C	60°C	1.01 m/s	3–4 mm	5%
1 mPa·s	10°C	60°C	1.01 m/s	5–6 mm	5%
1 mPa·s	10°C	60°C	1.01 m/s	7–8 mm	5%
1 mPa·s	10°C	60°C	1.01 m/s	9–10 mm	5%
1 mPa·s	10°C	60°C	0.5 m/s	5–6 mm	5%
1 mPa·s	10°C	60°C	0.7 m/s	5–6 mm	5%
1 mPa·s	10°C	60°C	0.9 m/s	5–6 mm	5%
1 mPa·s	10°C	60°C	1.1 m/s	5–6 mm	5%
1 mPa·s	10°C	60°C	1.3 m/s	5–6 mm	5%
1 mPa·s	10°C	60°C	1.01 m/s	5–6 mm	0%
1 mPa·s	10°C	60°C	1.01 m/s	5–6 mm	5%
1 mPa·s	10°C	60°C	1.01 m/s	5–6 mm	10%
1 mPa·s	10°C	60°C	1.01 m/s	5–6 mm	15%
1 mPa·s	10°C	60°C	1.01 m/s	5–6 mm	20%
1 mPa·s	10°C	40°C	1.01 m/s	5–6 mm	5%
1 mPa·s	10°C	45°C	1.01 m/s	5–6 mm	5%
1 mPa·s	10°C	50°C	1.01 m/s	5–6 mm	5%
1 mPa·s	10°C	55°C	1.01 m/s	5–6 mm	5%
1 mPa·s	10°C	60°C	1.01 m/s	5–6 mm	5%
2 mPa·s	10°C	60°C	1.01 m/s	5–6 mm	5%
4 mPa·s	10°C	60°C	1.01 m/s	5–6 mm	5%
6 mPa·s	10°C	60°C	1.01 m/s	5–6 mm	5%
8 mPa·s	10°C	60°C	1.01 m/s	5–6 mm	5%
10 mPa·s	10°C	60°C	1.01 m/s	5–6 mm	5%
1 mPa·s	5°C	60°C	1.01 m/s	5–6 mm	5%
1 mPa·s	10°C	60°C	1.01 m/s	5–6 mm	5%
1 mPa·s	15°C	60°C	1.01 m/s	5–6 mm	5%
1 mPa·s	20°C	60°C	1.01 m/s	5–6 mm	5%
1 mPa·s	25°C	60°C	1.01 m/s	5–6 mm	5%

References

1. Li WB, Zheng ZH, Fan DL, Wang YY, Bai Y. Analysis of oil and gas resource situation at home and abroad in the first half of 2025 and prospects. *China Min Mag.* 2025;34(8):9–15. (In Chinese).
2. Li GX, Lei ZD, Dong HW, Wang HY, Zheng XF, Tan J. Progress, challenges and prospects of unconventional oil and gas development of CNPC. *China Pet Explor.* 2022;27(1):1–11. (In Chinese). doi:10.3389/fenrg.2022.919966.
3. Hu W, Bao J, Hu B. Trend and progress in global oil and gas exploration. *Petrol Explor Dev.* 2013;40(4):439–43. doi:10.1016/s1876-3804(13)60055-5.

4. Fan DL, Wang ZL, Wang YY, Han ZQ, Li WB, Bai Y, et al. Analysis of oil and gas resources situation at home and abroad in 2024 and outlook. *China Min Mag.* 2025;34(1):46–54. (In Chinese). doi:10.1007/978-981-97-4756-6_1.
5. Wang FQ. China's oil and gas development enters the 10,000-meter era. *China Petrochem News.* 2025. (In Chinese). doi:10.28130/n.cnki.ncshb.2025.001037.
6. He D, Jia C, Zhao W, Xu F, Luo X, Liu W, et al. Research progress and key issues of ultra-deep oil and gas exploration in China. *Petrol Explor Dev.* 2023;50(6):1333–44. doi:10.1016/s1876-3804(24)60470-2.
7. Hao F. Enrichment mechanism and prospects of deep oil and gas. *Acta Geologica Sinica.* 2022;96(3):742–56. doi:10.1111/1755-6724.14961.
8. Wang H, Huang H, Bi W, Ji G, Zhou B, Zhuo L. Deep and ultra-deep oil and gas well drilling technologies: progress and prospect. *Nat Gas Ind B.* 2022;9(2):141–57. doi:10.1016/j.ngib.2021.08.019.
9. Zhang Z. Research on wellbore temperature distribution under complex conditions during drilling process [dissertation]. Chengdu, China: Southwest Petroleum University; 2019. (In Chinese). doi:10.27420/d.cnki.gxsys.2019.001111.
10. Jiang T, Sun X. Development of Keshen ultra-deep and ultra-high pressure gas reservoirs in the Kuqa foreland basin, Tarim Basin: understanding and technical countermeasures. *Nat Gas Ind B.* 2019;6(1):16–24. doi:10.1016/j.ngib.2019.01.003.
11. Lan P, Polychronopoulou K, Iaccino LL, Bao X, Polycarpou AA. Elevated-temperature and-pressure tribology of drilling fluids used in oil and gas extended-reach-drilling applications. *SPE J.* 2018;23(6):2339–50. doi:10.2118/191380-pa.
12. Li K. Influence of drilling fluid performance on drilling wellbore quality. *China Petrol Chem Stand Qual.* 2025;45(19):40–2. (In Chinese).
13. Liu J, Zhang T, Sun Y, Lin D, Feng X, Wang F. Insights into the high temperature-induced failure mechanism of bentonite in drilling fluid. *Chem Eng J.* 2022;445:136680. doi:10.1016/j.cej.2022.136680.
14. Kang YL, Wang KC, Xu CY, You LJ, Wang LM, Li N, et al. High-temperature aging property evaluation of lost circulation materials in deep and ultra-deep well drilling. *Acta Pet Sin.* 2019;40(2):215–23. (In Chinese).
15. Liu YM. Discussion on methods to improve high temperature resistance of logging instruments. *China Pet Chem Stand Qual.* 2020;40(3):119–20. (In Chinese).
16. Sun J, Yang J, Bai Y, Lyu K, Liu F. Research progress and development of deep and ultra-deep drilling fluid technology. *Petrol Explor Dev.* 2024;51(4):1022–34. doi:10.1016/S1876-3804(24)60522-7.
17. Zhang Y, Yin S, Mu H, Zhang X, Tan Q, Shao B. Study on the performance of lightweight roadway wall thermal insulation coating containing EP-GHB mixed ceramicsite. *Build Simul.* 2024;17(5):785–98. doi:10.1007/S12273-024-1105-X.
18. Raad H, Ali S, Faraj J, Castelain C, Chahine K, Khaled M. Enhancing photovoltaic performance through water-based cooling: a comprehensive review of passive and active techniques. *Appl Therm Eng.* 2026;283:128943. doi:10.1016/j.applthermaleng.2025.128943.
19. Shen S, Bu Y, Lu C, Liu S, Liu H, Guo S. Development and evaluation of insulation materials for deepwater cementing. *ACS Omega.* 2024;9(40):41904–13. doi:10.1021/acsomega.4c06759.
20. Tang S, Wei J, Song D. Research on active cooling technology of measuring instrument while drilling based on insulation tube in high temperature well. *Alex Eng J.* 2024;108:371–8. doi:10.1016/j.aej.2024.07.115.
21. Du Z, Gao M, Liu P, Wang P, Shi Y, Jiang S, et al. Multifunctional cement aerogel composites: ultralight, strong, and fire-resistant building insulation. *J Build Eng.* 2025;116:114628. doi:10.1016/j.jobe.2025.114628.
22. Fu C, Wang H, Zhan H, Li Y, Li S, Qiao Z, et al. Optimizing SiO₂-based thermal insulation materials via CSH/SiO₂ composite design: effects of synthesis conditions on phase composition, microstructure and properties. *J Alloys Compd.* 2025;1044:184347. doi:10.1016/j.jallcom.2025.184347.
23. Du X, Ran Y, Fan Y, Zhao Y, Shi X. Facile preparation of graphene aerogel as a thermal insulation material. *Fuller Nanotub Carbon Nanostruct.* 2025;33(2):178–85. doi:10.1080/1536383X.2024.2398806.

24. Scotti FM, Teixeira FR, da Silva LJ, de Araújo DB, Reis RP, Scotti A. Thermal management in WAAM through the CMT advanced process and an active cooling technique. *J Manuf Process*. 2020;57:23–35. doi:10.1016/j.jmapro.2020.06.007.
25. Zhang C, Sun JS, Huang XB, Lü KH, Wang JT, Li J, et al. Research progress and prospect of cooling technology for drilling fluid in deep and ultra-deep wells. *Chin J Eng*. 2025;47(6):1161–74. (In Chinese). doi:10.2139/ssrn.5394238.
26. Li M, Su Y. Preparation and properties of chitosan-based phase-change microencapsules for heat storage. *J Therm Anal Calorim*. 2025;150(26):21491–9. doi:10.1007/s10973-025-15051-5.
27. Su J, Li S, Tan Y. Performance evaluation and feasibility analysis of new phase change microcapsules in drilling fluid cooling. *Colloids Surf A Physicochem Eng Aspects*. 2025;722:137253. doi:10.1016/j.colsurfa.2025.137253.
28. Shi H, Wang J, Ni X, Zhang J, Li L, Zhang H, et al. Preparation and evaluation of phase-change microcapsules for drilling fluid cooling. *J Phys Conf Ser*. 2025;3043(1):012010. doi:10.1088/1742-6596/3043/1/012010.
29. Qi H, Chang S, Yang Y, Zhang H, Wu J. Experimental and numerical investigation of heat transfer physics in ice crystals melting. *Therm Sci Eng Prog*. 2025;61:103575. doi:10.1016/j.tsep.2025.103575.
30. Zhong F, Liu X, Chen J, Wei Z, Liu S, Yi X, et al. Experimental study on the melting characteristics of a suspended ice crystal based on new identification methods of ice-water interface and melting termination. *Int J Heat Fluid Flow*. 2024;110:109629. doi:10.1016/j.ijheatfluidflow.2024.109629.
31. Vispute DM, Baicu S, Stark L, Taylor MJ, Rabin Y. Multi-scale investigation of ice formation in CPA using calorimetry and cryomicroscopy. *Cryobiology*. 2025;121:105492. doi:10.1016/j.cryobiol.2025.105492.
32. Ekaykin AA, Veres AN, Kozachek AV, Lipenkov VY, Tebenkova NA, Turkeev AV, et al. The formation conditions of subglacial Lake Vostok's accreted ice based on its stable water isotope composition. *Problemy Arktiki I Antarktiki*. 2024;70(4):444–59. doi:10.30758/0555-2648-2024-70-4-444-459.
33. Huo Y, Yang D, Xie J, Yang Z. Effect of different freezing conditions on ice crystal formation behavior and ice-growth inhibition by cryoprotectants. *J Sci Food Agric*. 2024;104(14):8928–38. doi:10.1002/jsfa.13719.